RECLAMATION

Managing Water in the West

Optimization of Test Methods for Cathodic Protection Systems on Hydraulic Structures

Research and Development Office
Science and Technology Program
Final Report ST-2019-4108-01
Technical Memorandum No. 8540-2019-08

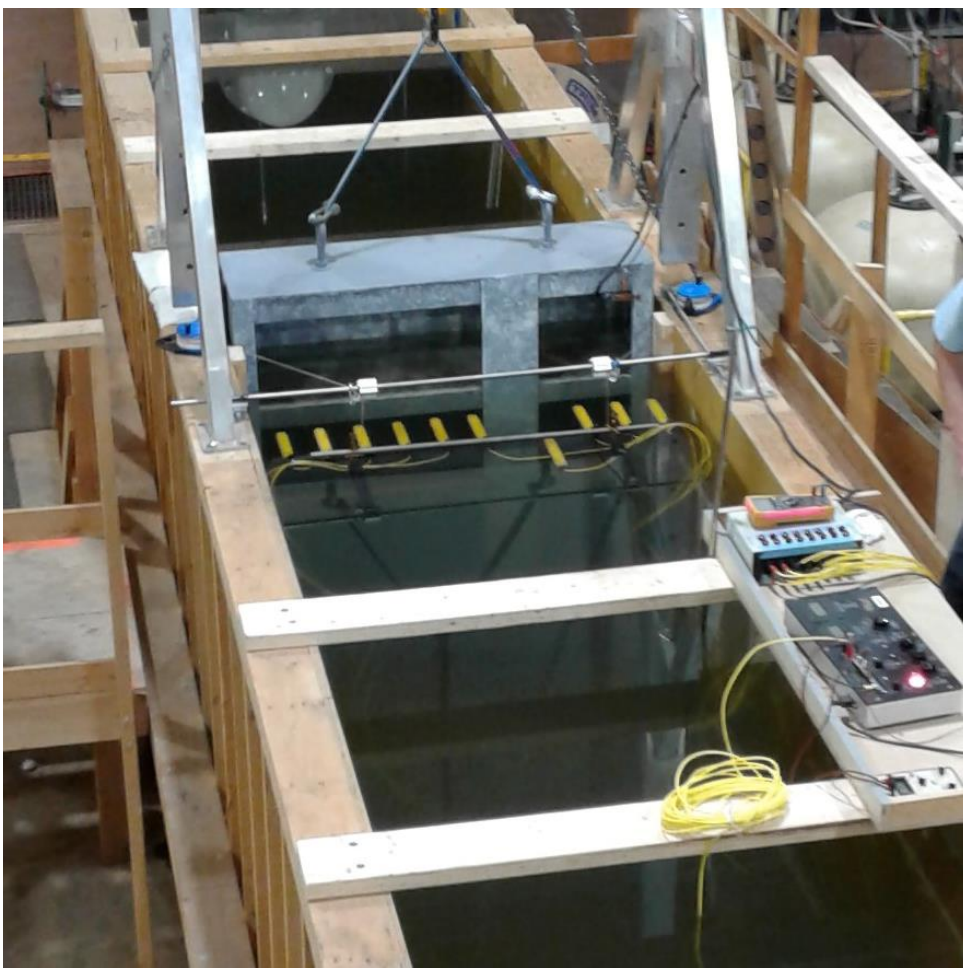

U.S. Department of the Interior
Bureau of Reclamation
Research and Development Office

June 2019

Mission Statements

The Department of the Interior conserves and manages the Nation's natural resources and cultural heritage for the benefit and enjoyment of the American people, provides scientific and other information about natural resources and natural hazards to address societal challenges and create opportunities for the American people, and honors the Nation's trust responsibilities or special commitments to American Indians, Alaska Natives, and affiliated island communities to help them prosper.

The mission of the Bureau of Reclamation is to manage, develop, and protect water and related resources in an environmentally and economically sound manner in the interest of the American public.

REPORT DOCUMENTATION PAGE		*Form Approved* *OMB No. 0704-0188*
1. REPORT DATE: JUNE 2019	**2. REPORT TYPE:** RESEARCH	**3. DATES COVERED** October 2015-June 2019
4. TITLE AND SUBTITLE Optimization of Test Methods for Cathodic Protection Systems on Hydraulic Structures		**5a. CONTRACT NUMBER** XXXR4524KS-RR4888FARD160100005
		5b. GRANT NUMBER
		5c. PROGRAM ELEMENT NUMBER 1541 (S&T)
6. AUTHOR(S) Jessica Torrey, Grace Weber Bureau of Reclamation Denver Federal Center PO Box 25007, MS 86-68540 Denver, CO 80225		**5d. PROJECT NUMBER** ST-2019-4108-01
		5e. TASK NUMBER
		5f. WORK UNIT NUMBER 86-68540
7. PERFORMING ORGANIZATION NAME(S) AND ADDRESS(ES) Bureau of Reclamation, Materials & Corrosion Laboratory PO Box 25007 (86-68540) Denver, Colorado 80225		**8. PERFORMING ORGANIZATION REPORT NUMBER** 8540-2019-08
9. SPONSORING / MONITORING AGENCY NAME(S) AND ADDRESS(ES) Research and Development Office U.S. Department of the Interior, Bureau of Reclamation, PO Box 25007, Denver CO 80225-0007		**10. SPONSOR/MONITOR'S ACRONYM(S)** **R&D:** Research and Development Office **BOR/USBR:** Bureau of Reclamation DOI: Department of the Interior
		11. SPONSOR/MONITOR'S REPORT NUMBER(S) ST-2019-4108-01
12. DISTRIBUTION / AVAILABILITY STATEMENT **Final report can be downloaded from Reclamation's website: https://www.usbr.gov/research/**		
13. SUPPLEMENTARY NOTES		

14. ABSTRACT *(Maximum 200 words)*

Proper design and installation followed by routine testing and maintenance of a corrosion mitigation system are key to maximizing the useful life of a protected structure. Researchers evaluated measurements crucial to the effectiveness and efficiency of cathodic protection systems on Reclamation's hydraulic steel gates. Factors inherent to cathodic protection on hydraulic steel structures were investigated: voltage drop between the structure and reference electrode; current shielding due to complex geometry of the structure, and placement of the reference electrode during testing.

15. SUBJECT TERMS

corrosion, cathodic protection, reference electrode, current shielding, IR drop, hydraulic steel infrastructure, photogrammetry

16. SECURITY CLASSIFICATION OF:			**17. LIMITATION OF ABSTRACT**	**18. NUMBER OF PAGES**	**19a. NAME OF RESPONSIBLE PERSON**
a. REPORT	**b. ABSTRACT**	**c. THIS PAGE**	U	43	Jessica Torrey
U	U	U			**19b. TELEPHONE NUMBER** 303-445-2376

S Standard Form 298 (Rev. 8/98)
P Prescribed by ANSI Std. 239-18

Bureau of Reclamation

Research and Development Office
Science and Technology Program

Materials and Corrosion Laboratory Group, 86-68540
Final Report ST-2019-4108-01
Technical Memorandum No. 8540-2019-08

Optimization of Test Methods for Cathodic Protection Systems on Hydraulic Structures

JESSICA TORREY Digitally signed by JESSICA TORREY
Date: 2019.07.09 15:51:35 -06'00'

Prepared by: Jessica Torrey, Ph.D.
Materials Engineer, Materials and Corrosion Laboratory Group, 86-68540

GRACE WEBER Digitally signed by GRACE WEBER
Date: 2019.07.10 09:34:54 -06'00'

Checked by: Grace Weber, M.S.
Materials Engineer, Materials and Corrosion Laboratory Group, 86-68540

BOBBI JO MERTEN Digitally signed by BOBBI JO MERTEN
Date: 2019.07.09 16:48:42 -06'00'

Technical Approval: Bobbi Jo Merten, Ph.D.
Coatings Specialist, Materials and Corrosion Laboratory Group, 86-68540

ALLEN SKAJA Digitally signed by ALLEN SKAJA
Date: 2019.07.09 15:11:49 -06'00'

Peer Review: Allen Skaja, Ph.D.
Coatings Specialist, Materials and Corrosion Laboratory Group, 86-68540

Acknowledgements

This research was funded through the Reclamation Science and Technology (S&T) Program project ID 4108. The following collaborators are acknowledged for knowledge sharing of their research outcomes and field implementation of state-of-the-art corrosion mitigation technology: Mike McInerney, Jonathan Trovillion, and Vince Hock from the U.S. Army Corp of Engineers Engineer Research and Development Center (USACE-ERDC), Construction Engineering Research Laboratory (CERL).

Notices

Acronyms and Abbreviations

3D	three dimensional
CERL	Construction Engineering Research Laboratory
CP	cathodic protection
CSE	copper-copper sulfate reference electrode
ERDC	Engineer Research and Development Center
ft	foot or feet
GACP	galvanic anode cathodic protection
HSS	hydraulic steel structures or hydraulic steel infrastructure
ICCP	Impressed current cathodic protection
in	inches
IR drop	voltage across a resistance when current is applied in accordance with Ohm's Law
mV	millivolt
Reclamation	Bureau of Reclamation
U.S.	United States
USACE	U.S. Army Corps of Engineers
V	volt
V_{OFF}	polarized potential or instant-OFF potential
V_{ON}	applied potential or ON potential

Executive Summary

The Bureau of Reclamation (Reclamation) has an estimated inventory of more than 1,000 cathodic protection (CP) systems on hundreds of projects across all five regions. The estimated value of these systems totals in the $20-30 million range, protecting assets that value well above the $1 billion mark. Proper design and installation followed by routine testing and maintenance of a corrosion mitigation system are key to maximizing the useful life of a protected structure. Reclamation and the U.S. Army Corps of Engineers (USACE) have a mutual interest in improving the effectiveness of CP systems on their respective hydraulic steel infrastructure (HSS). Reclamation staff collaborated with counterparts at the USACE Engineer Research and Development Center's (ERDC's) Construction Engineering Research Laboratory (CERL) to investigate various way of optimizing both the design and testing of CP systems.

Reclamation researchers evaluated measurements crucial to the effectiveness and efficiency of CP systems on Reclamation's hydraulic steel gates. The accurate measurement of the polarized potential on cathodically protected gates is the basis for system optimization and maintaining a long service life on the protected structure. Several factors inherent to CP on HSS were investigated: voltage drop between the structure and reference electrode, current shielding due to complex geometry of the structure, and placement of the reference electrode during testing. This report details the impact of these factors on CP applied to a laboratory-scale steel test gate with a vinyl coating. Parameters such as reference electrode location and anode location were varied, allowing researchers to observe the performance of the CP system based on polarized potential measurements. Researchers also utilized polarized potential mapping and photogrammetry with feature extraction to identify areas of corrosion.

The results of the testing did not show a significant impact of reference electrode placement on the polarized potential. In addition, placing the reference electrode close to the structure surface did not serve to eliminate the effects of IR drop, confirming that the bulk of the resistance in the circuit comes from the protective coating on the structure. Anode placement and shielding due to gate geometry was found to affect the polarized potential, but one that could be managed by proper CP system design and operation.

Potential mapping did not provide enough measurement precision to identify corroding regions of the gate. Photogrammetry, while useful in compiling a three-dimensional (3D) rendition of the gate as-built, also proved ineffectual in this case due to a fouling product that was similar in color to rust staining.

This study did not yield any findings that would change existing CP system testing practices. Reclamation facilities that manage hydraulic steel structure, such as gates, trashracks, or fish screens, with CP systems should continue to systematically test and adjust annually to meet polarized potential criteria using current interruption and the instant-OFF method. For direct-connect systems where the structure cannot be disconnected from the anode, indirect testing methods, such as an interruptible coupon, should be used for testing polarized potential. Visual inspections to identify areas of concern for corrosion should be conducted annually or when the structure is accessible.

Contents

Tables

Figures

Introduction

The Bureau of Reclamation (Reclamation) has an estimated inventory of more than 1,000 cathodic protection (CP) systems on hundreds of projects across all five regions. This includes both galvanic and impressed current CP systems on structures such as pipelines, tanks, gates, trash racks, and fittings. Many additional structures have other forms of corrosion mitigation such as protective coatings. The estimated value of these systems totals in the $20-30 million range, protecting assets that value well above the $1 billion mark.

Proper design and installation followed by routine testing and maintenance of a corrosion mitigation system are key to maximizing the useful life of a protected structure. Reclamation and the U.S. Army Corps of Engineers (USACE) have a mutual interest in improving the effectiveness of CP systems on their respective water infrastructure. In FY14, USACE funded Reclamation to identify critical corrosion monitoring needs and technical gaps relevant to Reclamation infrastructure.[1, 2] The two agencies jointly identified cross-agency priorities and complementary research tracks. Beginning in 2015, the USACE Engineer Research and Development Center’s (ERDC’s) Construction Engineering Research Laboratory (CERL) in Champaign, IL, conducted research on "Improved Effectiveness of Corrosion Prevention and Control Systems for HSS." Their effort used a combination of modeling and sensing to detect deficiencies in corrosion mitigation systems on submerged infrastructure, with miter gates as the model structure.[3-6]

The work conducted at USACE is two-fold: develop a tool to model individual structures to maximize the efficiency and protected area of a CP system upon installation and develop sensors to monitor the health of the coating and CP system through the lifetime of the structure. With this knowledge, corrosion mitigation systems could be installed and operated at their highest efficiency to prevent damage due to corrosion and extend the life of the structure. This approach could yield immediate benefit to Reclamation in both saved costs for repair and replacement of coatings or structure components, as well as provide a way to monitor the health of the corrosion mitigation system (coating and/or CP) without dewatering or removing the structure from service.

To complement the work being performed at USACE, Reclamation corrosion researchers investigated two topics under Reclamation’s Science and Technology Program: 1) the measurement of polarized potential on a test gate and 2) the phenomenon of cathodic disbondment for typical gate coatings. Investigations on polarized potential measurements are presented here; cathodic disbondment became the subject of a separate project.[7-9]

It is typical at Reclamation and USACE to install direct-connect galvanic anode CP (GACP) systems on gates. These systems use the principle of the galvanic series where a more active metal, such as magnesium, is electrically connected to the more noble structure metal, typically mild steel. The active metal will then become the anode for the structure and will sacrificially be consumed in the oxidation reaction to protect the structure metal, or cathode. These systems can be designed for a 20-year service life and require little maintenance. However, it is difficult to test their effectiveness in maintaining a protective polarized potential on the structure because the anodes cannot be disconnected from the system to eliminate the effects of voltage change due to circuit resistance, known as "IR drop." The researchers hypothesized that placing a reference electrode close to the surface of a structure could eliminate the IR-drop. The result would be an applied potential, or ON potential (V_{ON}), that is equal to the polarized potential, or instant-OFF potential (V_{OFF}). The outcome would be especially true at areas of coating damage, thus allowing accurate measurement of a structure's polarized potential with a direct-connect system. The researchers also evaluated the data to determine if standard reference electrodes placed close to a corroded surface would indicate: 1) the occurrence of corrosion based on the measured potential, 2) if shielding was occurring due to the structure geometry, and 3) if polarization maps could be generated to indicate areas of corrosion. Finally, researchers tested photogrammetry as a tool to generate three-dimensional (3D) maps of corrosion damage on a structure.

Effect of IR Drop

IR drop is defined as "the voltage across a resistance when current is applied in accordance with Ohm's law."[10] CP current flows towards the structure, and it is additive, making the measured potential on the structure appear more negative while current is flowing. The effect is that a structure appears to be better protected from corrosion than is true. Reducing the distance between the reference electrode and the structure decreases the IR drop for bare or poorly coated structures.[11] Gummow found that 95 percent of the IR drop between a holiday and remote earth will occur within a distance ten times the holiday diameter; everything outside that distance would be considered remote earth.[12] However, for most coated structures, the majority of the IR drop is due to the coating, and it is thus impractical to position a field reference electrode in that space unless the coating is significantly damaged.

If the only current producing the IR drop is the CP current, this current can be interrupted and a V_{OFF} measurement collected to provide the polarized potential of the protected structure. A V_{OFF} measurement is used to properly account for IR drop.[11] For an impressed current CP (ICCP) system, the rectifier output can then be adjusted to meet the desired nominal potential.[13] For a GACP system, additional anodes may be required. This study attempts to determine if the IR drop can be quantified and minimized for immersion service to make V_{OFF} measurements possible for a direct-connect anode system where the anode cannot be disconnected from the structure.

CP Current Shielding

To optimize corrosion prevention, a critical electrical potential must be maintained on all parts of the protected portion of the structure. This is achieved through distribution of anodes on the structure.[14] With ICCP anodes in particular, there is not a fixed guideline on anode positioning because the current output can be adjusted to meet the needs of the structure.[13] However, the geometry of the structure must also be considered as a factor when optimizing current distribution in CP systems. As Yi and Zhigang describe, it is possible for protection current to be blocked to certain parts of the structure by "adjacent structural surfaces," in an effect known as "shielding."[15] To minimize this effect, the number and distribution of anodes can be changed, although there is an optimum layout, after which there is a point of diminished returns due to increased installation work requirements and anode overconsumption.[15] Another option is to place anodes at "remote earth," or at such a significant distance from a structure where the current distribution on the structure is uniform. This study will investigate the effects of anode distance from a structure on geometric shielding and polarized potential.

CP Polarization Mapping

Evaluating the corrosion protection provided to a structure by CP involves measuring the structure's polarized potential with a reference electrode. Generally, the reference electrode placement is at a region of the structure that is most distant from anodes, i.e., where the lowest drop in potential would be expected.[13] In practice, if the region around a reference electrode meets potential requirements, the engineer assumes that the rest of the structure is also adequately polarized. However, the measured potential is primarily influenced by the electrical potential on the structure near the reference electrode. In practice, the surface of a steel structure is heterogeneous, and the use of multiple reference electrodes or a systematic grid survey measures the potential at each location on a structure to resolve local differences in polarized potential.[13]

Geometric or fabrication features on a structure, such as corners, edges, or crevices due to skip welding, are more susceptible to corrosion. A less negative than expected polarized potential in these areas may be an indication that corrosion is occurring. This study uses an array of commercially-available reference electrodes to map the polarized potential on the test gate, which includes the above-mentioned features, and shows how it varies with the reference electrode location. The results are interpreted using heat maps, illustrating the polarization gradients across the test gate. Areas with less negative potentials will then be inspected for corrosion. This indicates the sensitivity of the reference electrode and whether mapping of the potentials is a useful exercise for identifying corrosion on a structure in the field.

Photogrammetric Evaluation

As a direct source of data for corrosion mapping purposes, researchers investigated the application of photogrammetric evaluation with corrosion protection systems. Photogrammetry involves using a series of images to solve for the positions of individual points to create a 3D model. This model can then be subject to geometric analysis. Previous studies have shown that high resolution photogrammetric analysis can identify areas of visible corrosion, typically via color change from rust staining, on a steel surface.[16-18]

Experimental Procedure

Test Gate Construction and CP System Installation

To test the effectiveness of the corrosion monitoring systems, researchers fabricated a 4-foot (ft) wide by 6-ft tall bulkhead-style test gate out of mild steel panels (Appendix B). The steel panels were joined using the skip welding technique to intentionally create corrosion-susceptible locations at connections (Figure 1).

Figure 1. Bulkhead-style mild steel test gate (left) and a close-up of skip welding purposely performed to promote corrosion (right).

The test gate was coated with a zinc-rich vinyl primer and vinyl topcoats (USACE System 5-E-Z) following manufacturer recommendations. On the final coat, a speckle pattern was applied using the white vinyl topcoat to provide a contrasting optical texture for photogrammetry purposes (Figure 2).

A 4-ft wide by 30-ft long testing flume was outfitted for installation of the test gate by the addition of gate guides, an aluminum support frame, and a plexiglass viewing windows (Figure 3). The flume was sealed for water tightness. After the test gate was set in place, the flume was filled with water, and marks were made on the wall to indicate the minimum and maximum water levels with six inches (in) of allowable fluctuation. The water level was maintained between these marks for the duration of all tests.

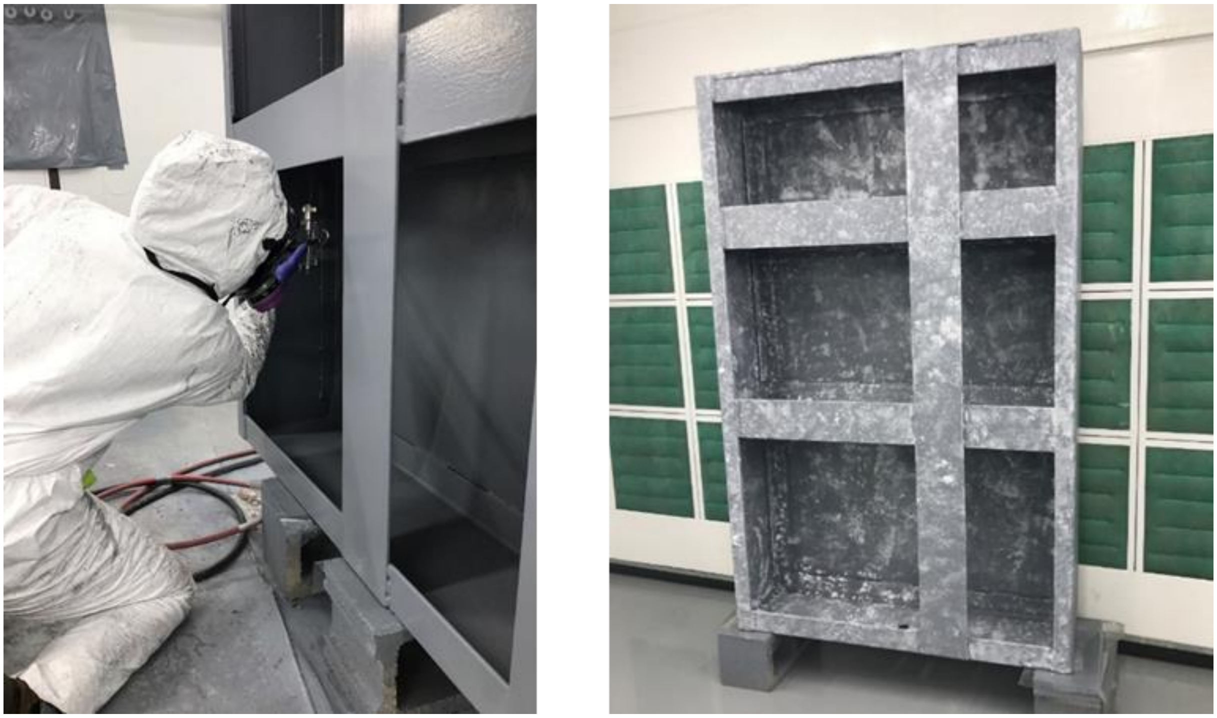

Figure 2. Vinyl coating application (left) and speckled pattern created with white topcoat (right).

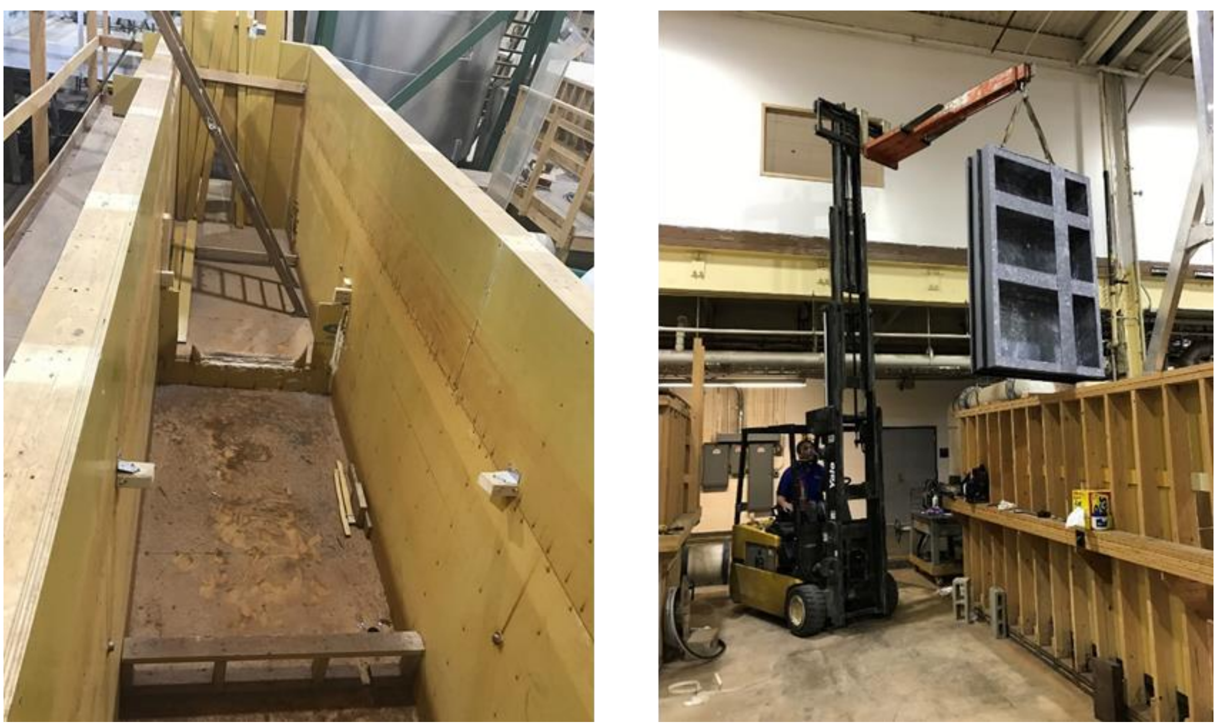

Figure 3. Testing flume during retrofit (left) and installation of test gate (right).

An ICCP system was installed on the test gate consisting of an 18-in platinum rod anode, power supply, and current interrupter. The evaluation procedure to record potentials on the test gate employed a custom-made array of ten copper-copper sulfate reference electrodes (CSEs) suitable for prolonged immersion service. The design included counterweights opposite the CSEs to keep the array level in the water. The array ensured that each CSE was equidistant from the steel surface it faced. One CSE, #4, was offset for positioning in front of the vertical steel brace of the gate, and all other CSEs were evenly distributed and set further forward for positioning at the interior of the test gate (Figure 4).

Figure 4. CSE array in dewatered test gate (left) and submerged at the bottom of flume (right).

The CSE array was suspended from a pulley system which allowed the array to be vertically positioned spanning the entire immersed gate height. A rail system allowed the array to be moved horizontally into the frame of the gate, i.e., the “IN” position. The ten CSEs in the array also spanned the full width of the gate (Figure 4). This combination of vertical and horizontal mobility allowed researchers to record the polarized potential at several different regions of the gate over the duration of each experiment. By moving the reference electrode array closer to and further from the test gate, researchers observed differences between localized and general effects of corrosion on potential measurements.

Polarization Tests

Two experiments were performed to test each corrosion prevention and control method. The first experiment, the "Fixed Anode Test," fixed the anode position at a specific distance from the gate and performed regular measurements of the gate potential. In the second experiment, the "Moving Anode Test," the anode position varied, and regular measurements occurred over a 46-day period.

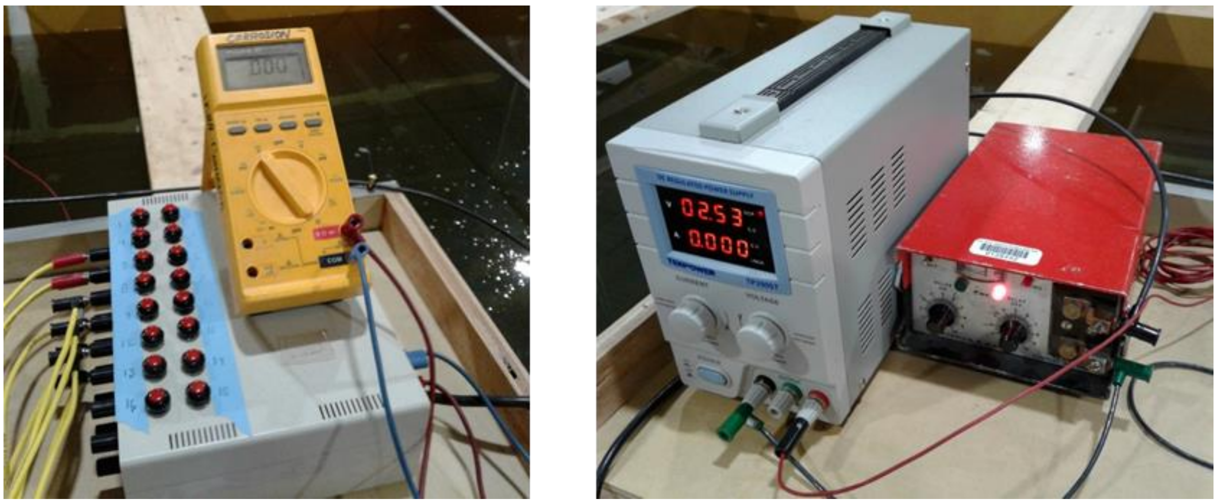

Figure 5. Equipment used to take potential measurements (left) and power supply with current interrupter wired into circuit (right).

Potentials were recorded from CSEs attached to a switch box to activate each electrode (Figure 5). V_{ON} was measured using a high impedance multimeter and taken with current flowing to the test gate. A current interrupter was included in the circuit between the power supply and the anode to facilitate measuring V_{OFF}. V_{OFF} was measured using the same high impedance multimeter, recording the meter output value approximately 300 milliseconds after interrupting the current to the gate. The employed technique is typical of field data collection and is often described as the recording the second drop in the multimeter readings after interruption. The current interrupter cycle was set for ten seconds with current on followed by three seconds with current off. The system output was adjusted after completing each set of measurements so that the polarized potential at the least negative location on the gate equaled the NACE criteria for sufficient CP of -850 millivolt (mV) with respect to a CSE (mV_{CSE}).[19]

Fixed Anode Test Method

The Fixed Anode Test fixed the anode position at eight feet from the gate. The evaluation consisted of collecting data 30 times over a 40-day period; measurements were taken more often in the first seven days and approximately three times per week for the remainder of the experiment. The CSE placement included ten vertical positions (Z and A-I), ten horizontal positions (1-10), and three lateral positions (IN, MID, and OUT), for a total of 300 measurement positions (Figure 6). The first 12 data collections, taken during the first seven days of testing, recorded only the V_{ON} at each CSE position. The final 18 data collections, taken from days 8 through 40, recorded both the V_{ON} and V_{OFF}.

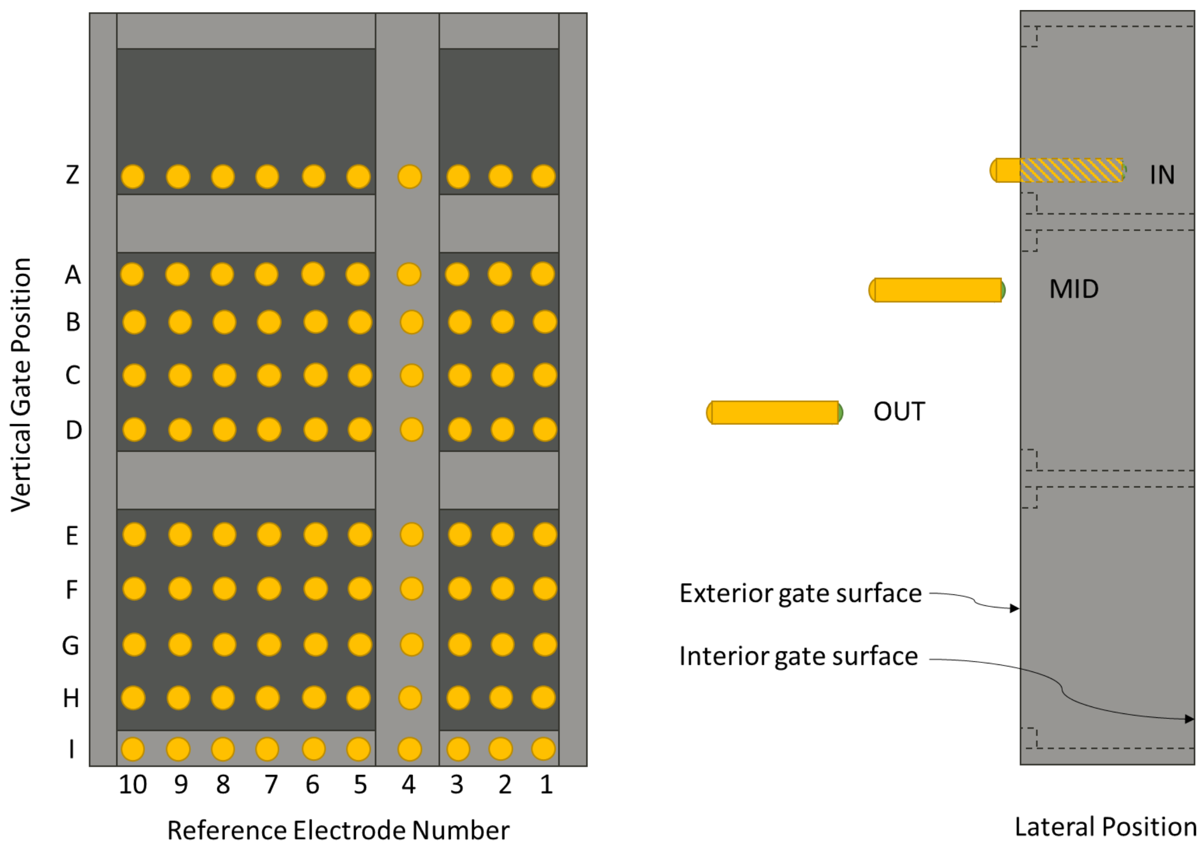

Figure 6. Schematic of CSE positions with respect to the 4 ft x 6 ft test gate: vertical positions Z and A-I, horizontal positions 1-10, and lateral positions IN, MID, and OUT.

The three lateral measurement positions are IN, MID, and OUT. The OUT position placed the reference electrode array so that the end of the reference was approximately 8 in from the exterior surface of the gate. The MID position placed the end of the CSEs approximately 0.5 in from the exterior surface. The IN position placed the CSEs as close to the interior gate surface as allowed by the array. Potential measurement at position I for the IN position was not possible due to the obstructing support beam of the test gate. Similarly, CSE #4 overlapped the vertical brace on the exterior surface of the gate and was positioned further back in the array than the other CSEs so that at the IN position, CSE #4 was just off the surface of the brace.

Moving Anode Test Method

The Moving Anode Test evaluated six anode positions, and researchers collected data 22 times at regular intervals over a duration of 46 days. The reference electrode array placement included three vertical positions (Z, D, and H), ten horizontal positions (1-10), and two lateral positions

(IN and OUT), for a total of 60 measurement positions. These positions aligned with the correspondingly designated positions in Figure 6.

The initial anode position was 10 ft away from the test gate, and both the V_{ON} and V_{OFF} were recorded at each CSE position, again using a switch box to activate each CSE and a high impedance multimeter to record data as described above. Beginning on the tenth day, the anode was moved 2 ft closer to the test gate at six-day intervals until the anode was positioned just off the surface of the gate.

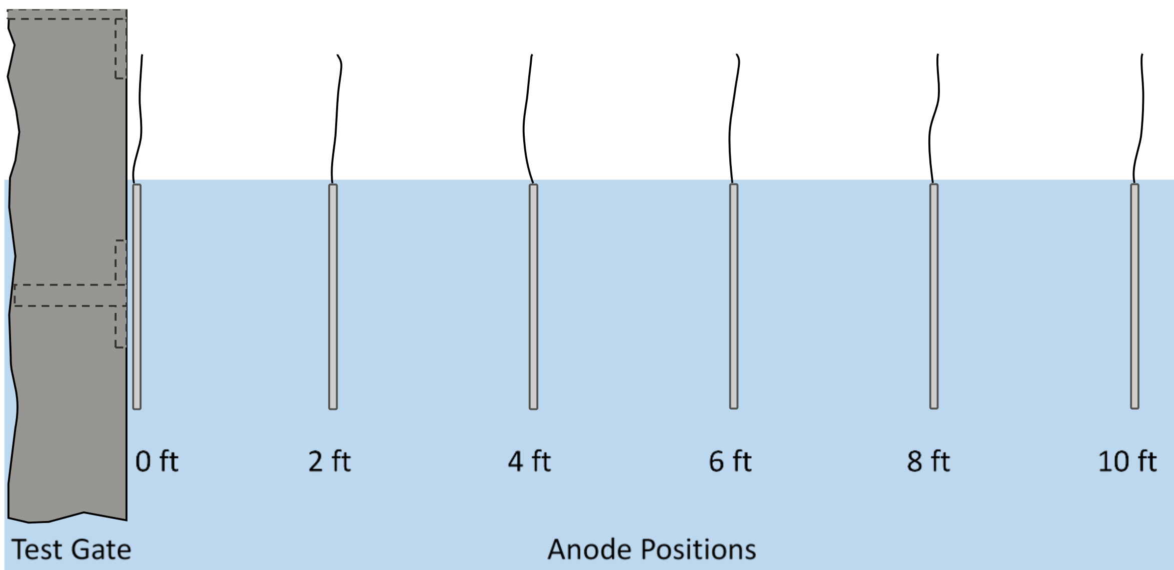

Figure 7. Moving Anode Test anode positions. The platinum anode is 18 in long; the test gate is 6 ft high (full height not shown).

Photogrammetric Evaluation

During this investigation, images of the steel test gate were captured before and after immersion with the intention of using feature extraction software to identify areas of corrosion. A 3D, scaled, geometric model of the gate was created using photogrammetric evaluation. Photos of the external portions of the steel test gate were taken using a Sony A7r mirrorless full-frame camera with 35 mm lens. For easier image capture of the interior compartments, 360-degree photographs were captured using a Nikon KeyMission 360 spherical camera. The series of images that were captured of the gate were then used to solve for the positions of individual points, yielding a geometric analysis, or point cloud model, of the gate.

Results and Discussion

Researchers conducted the above-described measurements to discover ways to improve the effectiveness and efficiency of CP systems on Reclamation's hydraulic steel gates. Several factors inherent to CP on HSS were investigated: voltage drop between the structure and reference electrode; current shielding due to complex geometry of the structure, and placement of the reference electrode during testing. The following discusses the results of these experiments and their impact on CP of a laboratory-scale steel test gate with a vinyl coating.

Effect of IR Drop

The effects of voltage drop through the electrolyte and coating were discerned by measuring V_{ON} and V_{OFF} at many reference electrode array positions relative to the test gate. Measurements typically occurred twice per day for the first week of the Fixed Anode Test. The measured values stabilized as the polarization of the gate progressed. This resulted in a series of reductions to the measurement frequency, to once per day, several times per week, and then every few weeks, as reflected in Figure 8. The figure presents the Fixed Anode Test results for only the vertical positions Z, D, and H, and it shows V_{ON} and V_{OFF} in mV, i.e., mV_{ON} and mV_{OFF}, respectively, in accordance with standard convention and for discussion purposes of the small voltage changes.

There was a spike in the V_{ON} for the test gate between Day 7 and Day 8 of the Fixed Anode Test. On this day, the test methodology changed from measuring only V_{ON} to measuring both V_{ON} and V_{OFF} on Day 8 and for each successive day of the Fixed Anode Test. This can be accounted for by the adjustment in applied potential to bring the polarized potential to meet -850 mV_{CSE} criteria.

In general, both V_{ON} and V_{OFF} remained consistent across all CSE positions. However, several trends are apparent in the Fixed Anode Test data (Figure 8): 1) V_{ON} becomes less negative as the distance to the interior of the test gate decreases, 2) conversely, V_{OFF} becomes more negative as this distance decreases, and 3) the effect is less pronounced for CSE #4, with its results being most approximate to the OUT position for the other CSEs. The effect also appears to be more pronounced closer to the water surface, i.e., vertical position Z. The results of the other vertical or horizontal positions are consistent with these observations, and, therefore, the data is not shown. Average values for V_{ON} and V_{OFF} at representative CSE positions for OUT, MID, and IN lateral positions and additional statistics are included in Appendix A – Table I.

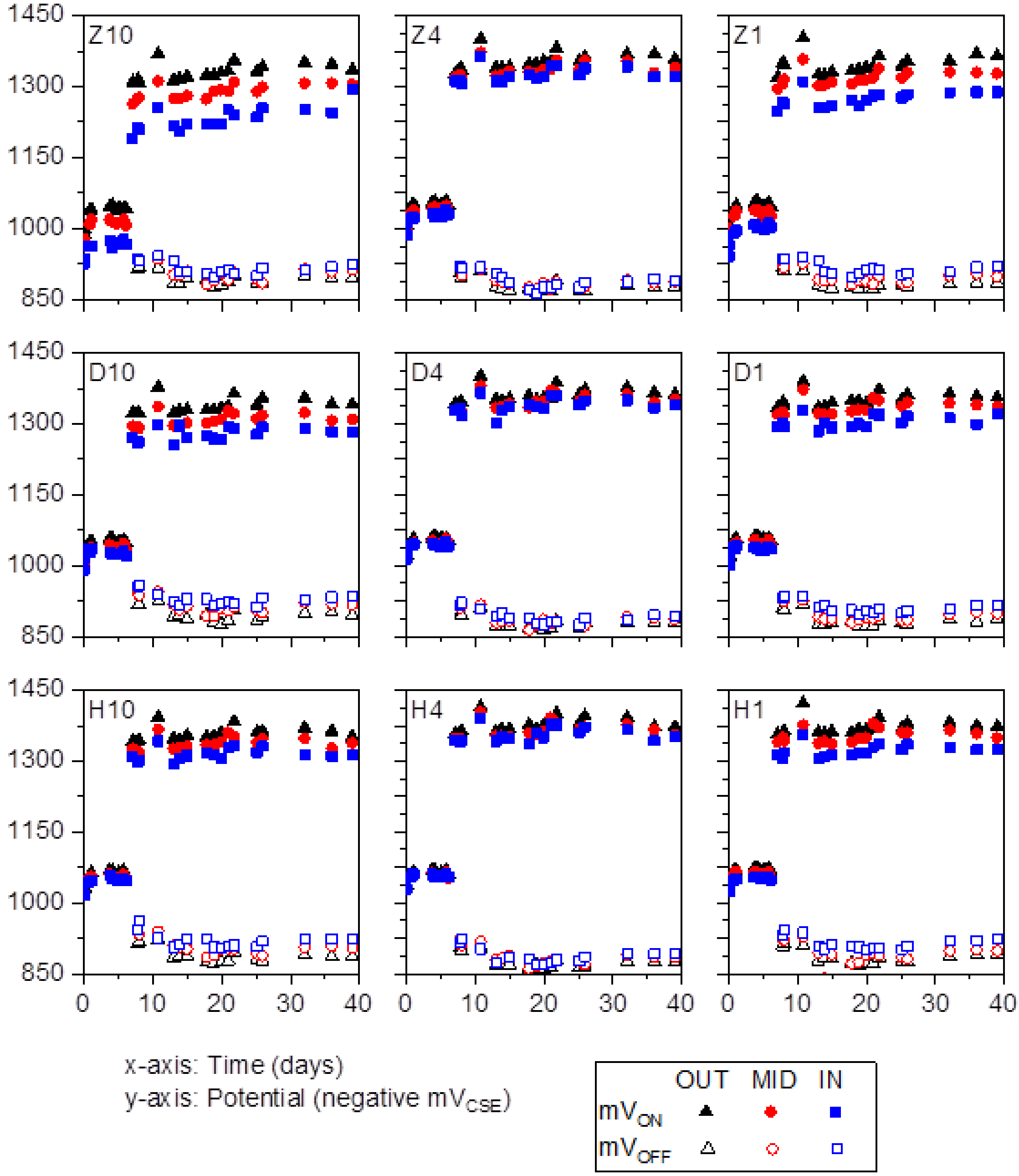

Figure 8. Fixed Anode Test results for V_{ON} and V_{OFF} at representative CSE locations.

As expected, the difference between V_{ON} and V_{OFF}, which is the IR drop, decreases as the distance to the interior of the test gate decreases. For example, the IR drop is greatest for the OUT position and became smaller as the CSE array moved to the MID and IN positions in Figure 8. This was due both to the V_{ON} tending to become less negative moving from the OUT to IN positions and the V_{OFF} becoming more negative. The shifting of V_{OFF} was not expected;

further clarification is needed and could be investigated with fixed reference electrodes at each position to measure the local depolarization curve.

The average IR drop for all positions combined was 319 mV. This reinforces the importance of measuring V_{OFF} rather than V_{ON} to demonstrate that a CP system is functioning properly and polarizing the structure to meet CP criterion.

CSE #4 showed the least variation between the IN, MID, and OUT lateral positions. This may be a result of CSE #4 being positioned over a vertical steel brace. All other CSEs in the electrode array are within the structure of the test gate for the IN position except CSE #4, which remains just off the surface of the vertical brace.

There is also a correlation between vertical position of the CSE and the IR drop, with IR drop increasing as the depth of water immersion increased. This is mainly due to the V_{ON} becoming more negative; V_{OFF} remained consistent for each vertical position. It should be noted that the anode was located at the water line, so the top-center of the gate would be approximately 14.5 in closer to the anode than the bottom-center of the gate and thus, have a lower resistance component from the electrolyte.

CP Shielding and Polarization Mapping

The effects of current shielding were determined for the Fixed Anode Test by constructing polarization heat maps showing V_{OFF} at the IN, MID, and OUT lateral positions at Day 20 of the experiment (Figure 9). The first observation for these heat maps is that the CSE positions associated with CSE #4 and, to a lesser extent, position I are the least negative. These are the positions located directly adjacent to structural steel braces. This result is somewhat counterintuitive since it would be expected that these braces see the least amount of current shielding on the structure, and thus be more polarized, as is the case with CSE positions D and H which sit just above the horizontal braces.

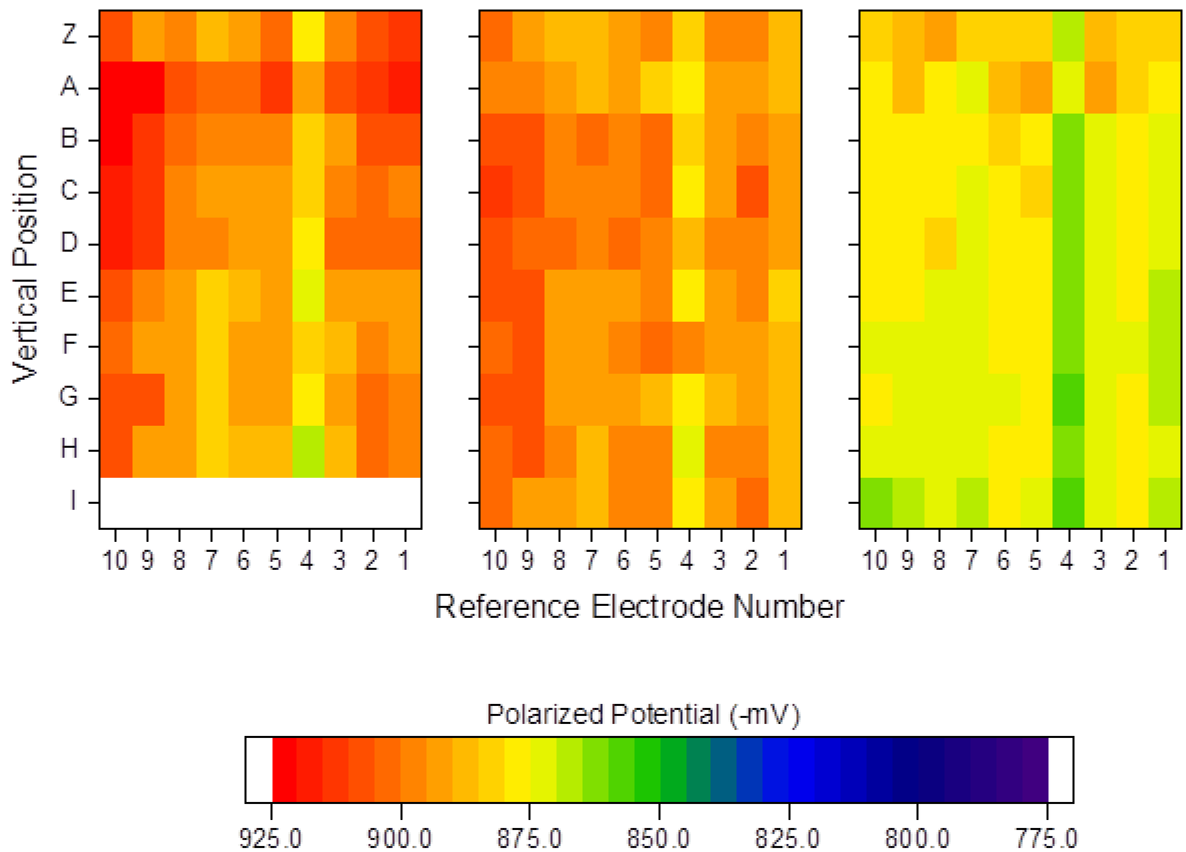

Figure 9. Fixed Anode Test results for Day 20 showing V_{OFF} at the IN, MID, and OUT positions (left to right); no data available for position I, IN due to obstructing structural support.

Generally, the right side of the gate, at CSEs 1-4, is less polarized than the left-most positions on the gate. This could be because there is approximately 18% more surface area on the right side of the gate. In addition, the vertical brace right of center could be acting as a current shield for the far right of the gate.

Position Z and A at the top of the test gate are more polarized than positions I and H at the bottom. This follows the convention that current density, and thus polarization, will be inversely proportional to the distance from the anode. In this case, the anode is located at the water surface eight feet from the gate, so the top of the gate would be closer to the anode than the bottom of the gate, as previously mentioned.

The effects of current shielding were determined in the Moving Anode Test by varying anode position relative to the test gate and measuring V_{ON} and V_{OFF} at both the IN and OUT lateral positions. Average results for each anode position for the entire test duration (46 days) at each CSE position are presented graphically in Figure 10. (only vertical positions Z, D, and H were measured during the Moving Anode Test). Average values for V_{ON} and V_{OFF} at representative CSE positions for OUT and IN lateral positions and additional statistics are also included in Appendix A – Table II. Again, V_{ON} and V_{OFF} remained consistent across all CSE positions.

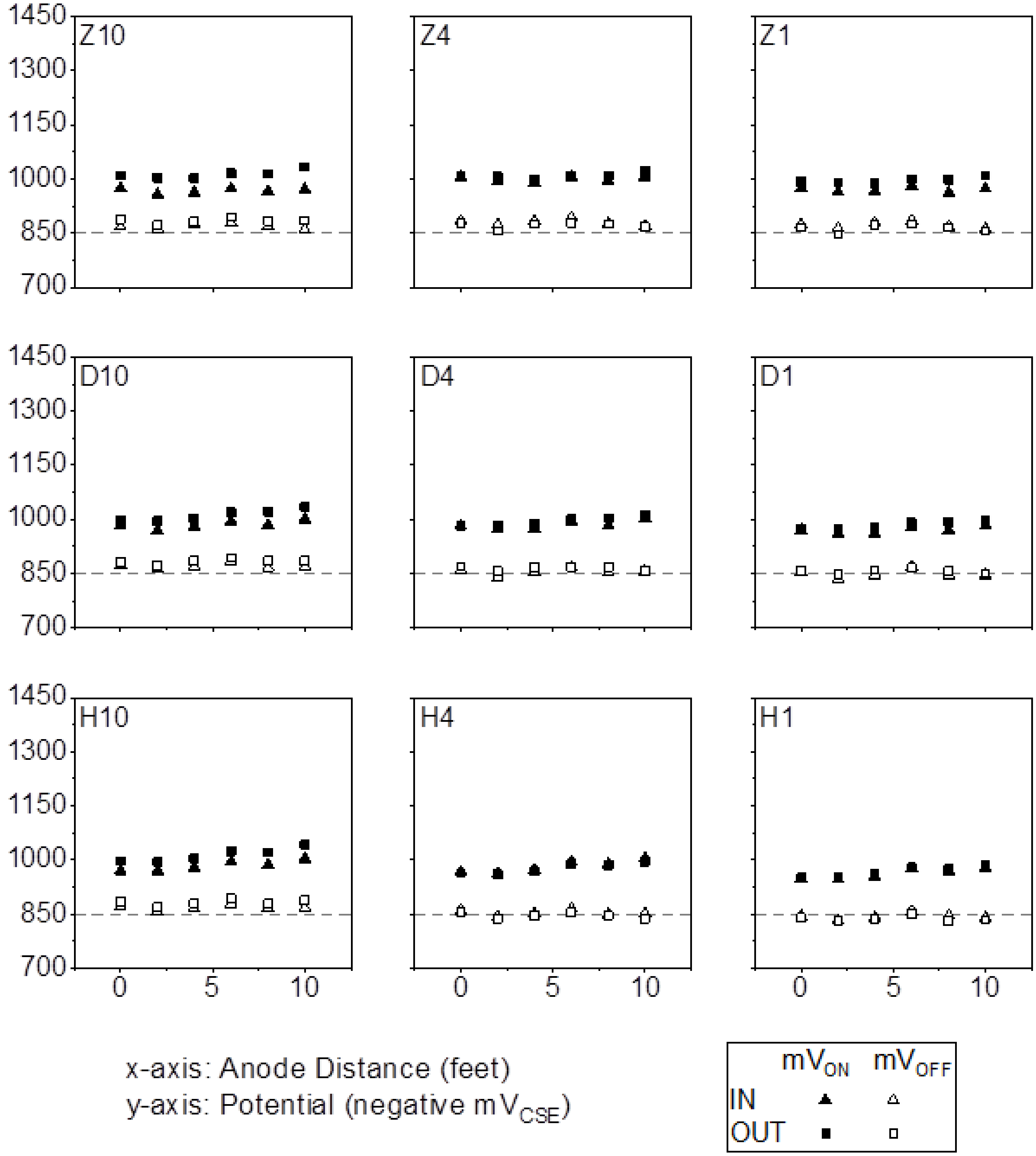

Figure 10. Moving Anode Test average VON and VOFF for representative CSEs at each investigated anode distance from the gate, including a dashed line for the NACE -850 mVCSE criteria.

The OUT position tended to have a more negative value than the IN position for both V_{ON} and, to a lesser extent, V_{OFF}. This difference was most pronounced when the CSE was close to the water surface, corresponding to a location where the anode was closest to the gate (anode is at water surface). The IR drop followed the same trend, with the OUT position having a larger differential, likely because the CSE is further from the gate surface and thus the IR drop is larger due to a larger resistance contribution from the electrolyte. Although the average V_{OFF} for the gate met NACE criteria of -850 mV_{CSE} or more negative, the lower right-hand corner of the gate, positions D1 and H1, did not consistently meet criteria (Figure 10).[19] As noted in the Fixed Anode Test, this is the location furthest from the anode and with the most structural braces in proximity.

Heat maps were constructed to provide a visual representation of V_{OFF} at one point in time. Researchers hoped to correlate differing V_{OFF} values with corrosion found through a visual inspection. Figure 11 shows heat maps with V_{OFF} measurements at the IN position, and Figure 12 shows heat maps with measurements at the OUT position. Each heat map represents the gate polarization gradients, i.e., V_{OFF}, at a unique anode position just before moving the anode to the next position. Results shown are for Day 6 except for the 10 ft anode position, which is Day 4 because Day 6 testing did not occur at this anode position. The Day 4 values at the 10 ft position closely reflected the other heat maps, allowing for a side-by-side comparison with the other data.

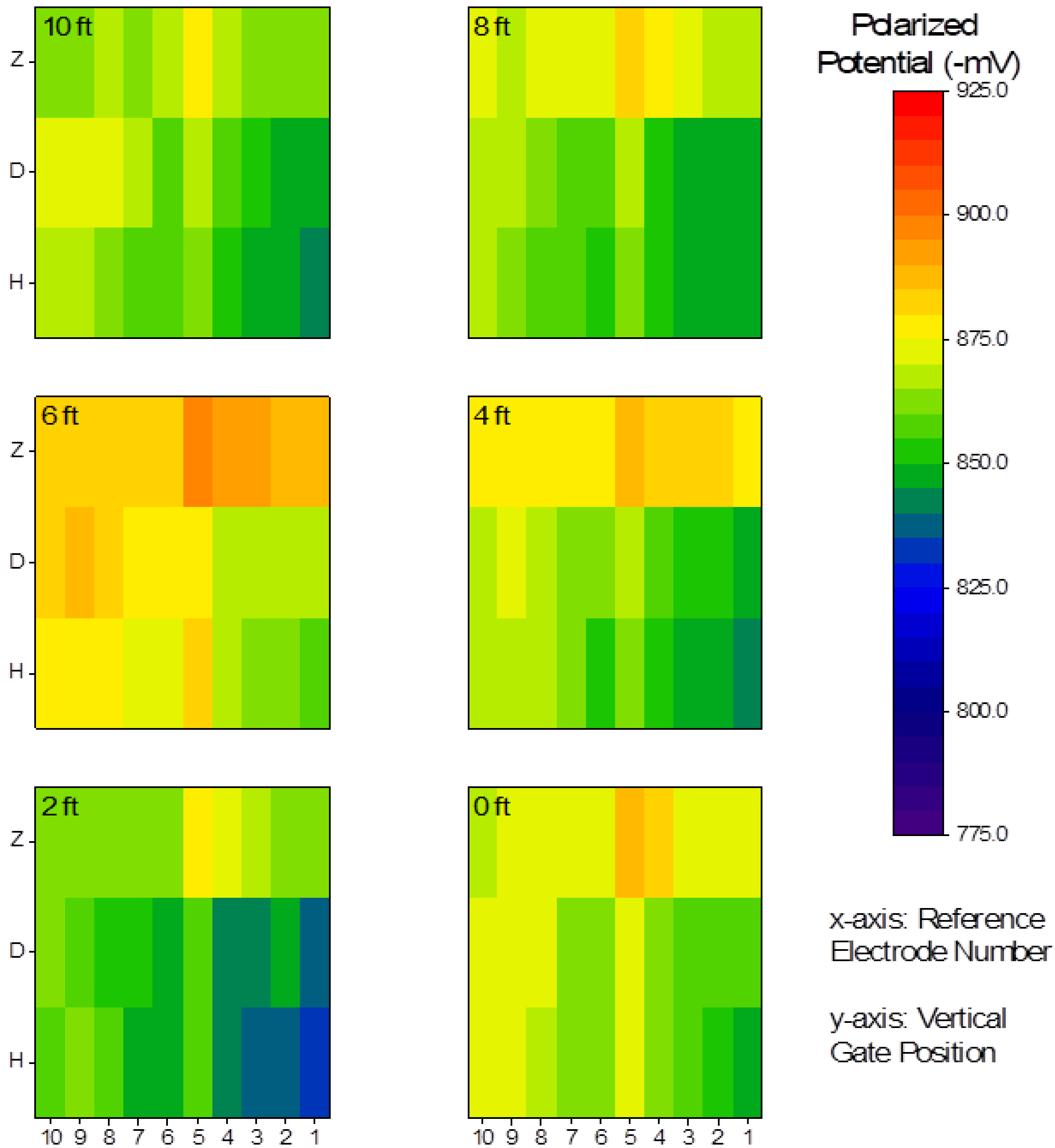

Figure 11. Moving Anode Test heat maps showing V_{OFF} at the IN position for each investigated anode distance from the gate; Day 6 data shown for all positions except 10 ft (collected at Day 4).

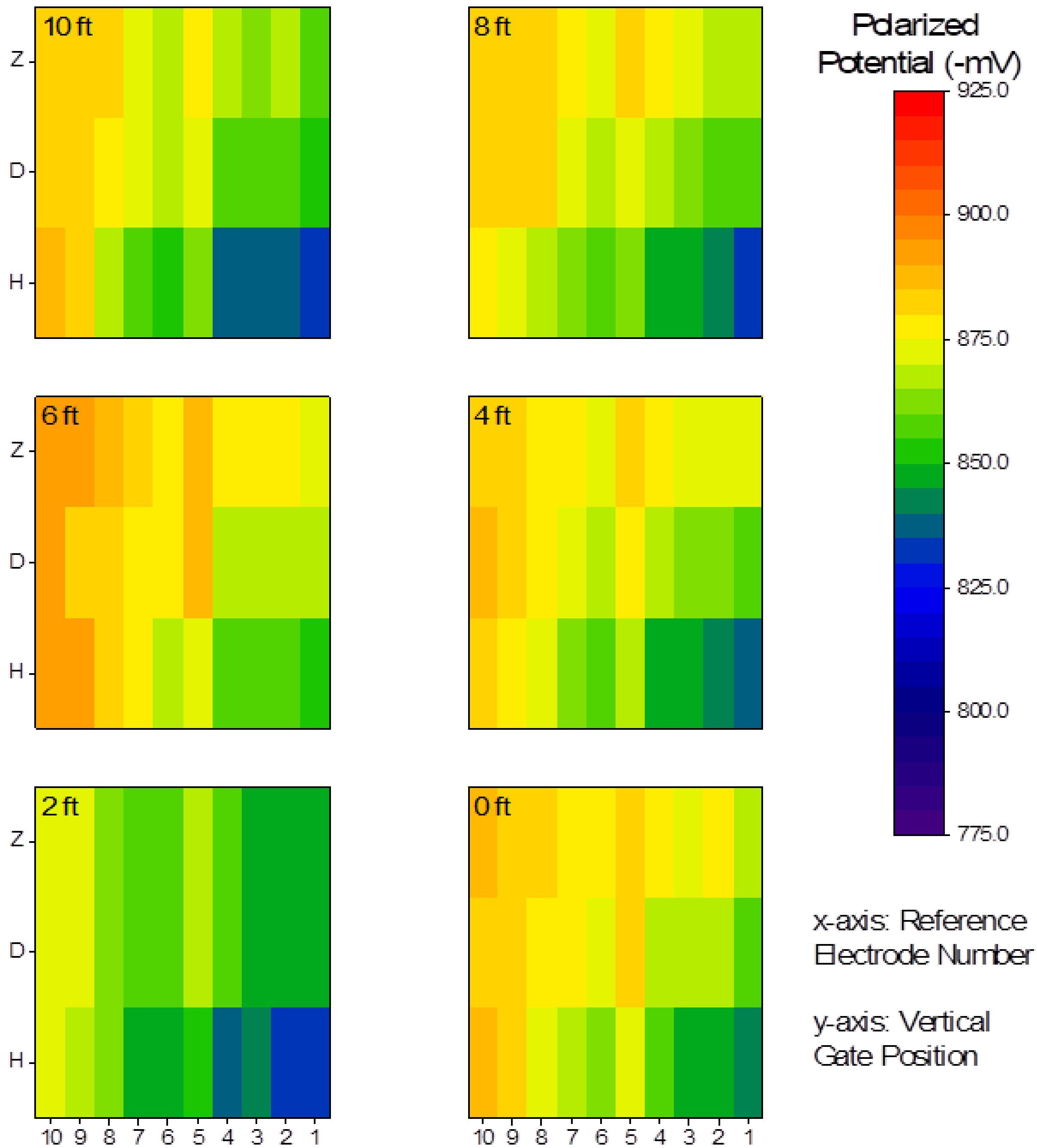

Figure 12. Moving Anode Test heat maps showing V_{OFF} at the OUT position for each investigated anode distance from the gate; Day 6 data shown for all positions except 10 ft (collected at Day 4).

The OUT position heat maps (Figure 12) reveal that the polarized potential tends to be more negative on the left side of the test gate and less negative in the lower right corner of the gate. This shows that the vertical brace to the right of center causes shielding of CSE positions 1-3. CSE #5 exhibits a significantly more negative polarized potential than the adjacent electrodes. This suggests that it is picking up additional polarization from the proximate corners and edges of the vertical brace. This is consistent with literature where computer simulations have shown that the maximum CP current is found at geometric features such as corners and edges.[20] CSE #3 does not show this effect, likely due to the edges to the right of the brace being shielded from receiving as much current from the centered anode.

The V_{OFF} at position Z in both Figure 11 and Figure 12, which is the closest vertical position to the anode, measured more negative than position H, at the bottom of the gate. Additionally, the lower right corner of the gate is the least polarized region of the gate. This supports the assertion that the polarized potential is affected by shielding and current concentrations due to geometric features, as well as an effect of distance from the anode with the locations farthest away receiving the least amount of CP current.

This effect of a polarization gradient is more significant for the OUT measurements (Figure 12) than for the IN measurements (Figure 11). The OUT position is what is typically measured in a field setting, where a reference electrode is lowered from the top of the gate to a specific depth below waterline at a distance 6-12 in ahead of the gate. This suggests that field measurements made with the reference electrode further from the structure instead of in the structural compartments could be collecting a global estimate which both under- and over-estimates the true polarized potential on different sections of the gate. However, the difference in the values is small enough — 9 mV less negative in the OUT position than the IN position for H1, and 12 mV more negative in the OUT position than the IN position for Z10, averaged across all anode distances — that a corresponding remedial action to bring the underpolarized areas above criteria would not result in overpolarization of other parts of the structure.

In all heat maps, the lower right corner of the gate tends to have a less negative polarized potential, indicated by the cooler color in this area. These results were compared to visual inspection of that location (Figure 13, Figure 14). The front lower right corner did not appear to have significant corrosion damage, with most of the discoloration in the examination due to fouling product. The back lower right corner, however, had significant rust staining in all the skip welds. It could not be determined that this was the causing factor for the less negative polarized potentials that were measured. The shielding and anode proximity effects discussed above likely have more weight on the observed polarizations in this location.

Figure 13. Photos of the front lower right corner of the test gate. Little corrosion can be seen, with most of the discoloration attributed to fouling.

Figure 14. Photo of the back lower right corner of the test gate. Corrosion staining can be seen in the crevices that are present due to skip welding.

Photogrammetry

After creating 3D geometric models of the test gate, researchers utilized feature extraction to highlight suspected corrosion areas on the post-immersion model (Figure 15). First, a point on the model within an area known to be corrosion product was chosen to provide a color reference. The feature extraction software then searched the model for other similarly-colored areas within a certain RGB value range. These areas are highlighted on the model, as shown in the rightmost image in Figure 15. In practice, however, the corrosion product may be the same color as other non-corrosion deposits that form or collect on the surface and may not always be representative of corrosion. In the example shown in Figure 16, there was corrosion detected in the corners and edges of some welds (see right hand side corresponding to skip welds in Figure 14), but the software also identified fouling deposits on the bottoms of the compartments as corrosion. This illustrates the need for a clean surface or optically-distinguishable rust staining when using photogrammetry to identify corrosion. In practice, it may require pressure washing or other methods to clean a gate that has been in immersion service for many years before photogrammetry could be employed.

Figure 15. Isometric view of each model: uncoated, coated before immersion, and coated after immersion with corrosion highlighted in brown (from left to right).

Figure 16: Feature extraction for corrosion in lower compartment of gate with corrosion highlighted as pink; the analysis could not differentiate between rusting staining and fouling.

Conclusions

This study focused on measurements crucial to the effectiveness and efficiency of CP systems on Reclamation's hydraulic steel gates. The accurate measurement of the polarized potential on cathodically protected gates is the basis for system optimization and maintaining a long service life on the protected structure. A laboratory-scale test gate was fabricated to investigate both the reference electrode and anode positions with relation to the structure and their effect on IR drop and current shielding. Polarized potential mapping and photogrammetric evaluation with feature extraction was also performed to identify areas of corrosion.

The results of the testing did not show a significant impact of reference electrode placement on the polarized potential. In addition, placing the reference electrode close to the structure surface did not serve to eliminate the effects of IR drop. This holds with conventional wisdom in testing of buried structures that the bulk of the resistance in the circuit comes from the protective coating on the structure. This leads to the conclusion that polarized potential cannot be directly measured for direct-connect systems; indirect testing methods, such as an interruptible coupon, would need to be used. These test coupons should be in areas of the gate likely to have the lowest polarized potential, e.g., areas with complex geometry and located far from the anode. Anode placement and shielding due to gate geometry was not found to have a large effect on the polarized potential.

Potential mapping did not result in enough precision of measurement to identify corroding regions of the gate. Photogrammetry, while useful in compiling a 3D rendition of the gate as-built, proved ineffectual in this case due to a fouling product that was similar in color to rust staining.

Recommendations

This study did not yield any findings that would change the way CP systems are tested. Reclamation facilities that manage hydraulic steel structure, such as gates, trashracks, or fish screens, with CP systems should continue to systematically test their CP system using the following principles:

- test each system annually at approximately the same time each year,
- interrupt the current source to measure a polarized potential that accounts for the IR drop in the system,
- where interruption between the anode and the structure is not possible, e.g. for direct-connect systems, a test coupon could be installed with an interruptible connection to the structure,
- test large structures in a grid pattern with upstream and downstream sides tested separately,
- test with the reference electrode within two feet of the structure, where possible,
- adjust the current source to meet a polarized potential (V_{OFF}) of -850 mV_{CSE} or more negative and not more negative than -1200 mV_{CSE},
- visual inspection for signs of corrosion and coating damage should accompany potential testing, where possible.

Reclamation engineers that design corrosion protection systems for hydraulic steel structures should consider:

- that this study found evidence of current shielding even on the relatively simplistic geometry of the test gate,
- anode placement when designing a CP system should account for both the geometry of the structure and the distance from the anode.

References

1 J. Torrey, R. Turcotte, "2014 Overview of Bureau of Reclamation Corrosion and Mitigation Issues," U.S. Department of the Interior Bureau of Reclamation, Technical Memoradum No. MERL-2014-83, 2014.

2 M.K. McInerney, C.P. Marsh, V.F. Hock, T.A. Carlson, "A Survey of Corrosion and the Conditions of Corrosion Protection Systems in the U.S. Army Corps of Engineers," U.S. Army Corps of Engineers, ERDC/CHL CHETN-IX-39, 2014.

3 C. Marsh, A. Navarro, R. Weber, T. Carlson, V. Hock, M. McInerney, "Combined Structure Geometry and Anode Placement Effects on Cathodic Protection Effectiveness," *Materials Performance and Characterization* 6, 1 (2017): p. 292.

4 T.A. Carlson, A.P. Friedl, C.P. Marsh, J.P. Miller, J.B. Bushman, R. Bushman, B. Phull, S., "Polarization Decay Fit for Assured Cathodic Protection of Steel Structures," U.S. Army Corps of Engineers Engineer Research and Development Center, ERDC/CERL TR-16-20, 2016.

5 M. McInerney, C. Marsh, H. Hock, A. Beitelman, A. Skaja, T. Carlson, "Use of Coatings on Hydraulic Steel Structures: Part 2 – Supplemental Information," U.S. Army Corps of Engineers, ERDC/CHL CHETN-IX-44, 2016.

6 M. McInerney, C. Marsh, H. Hock, A. Beitelman, A. Skaja, T. Carlson, "Use of Coatings on Hydraulic Steel Structures: Part 1 – Overview and Field Survey," U.S. Army Corps of Engineers, ERDC/CHL CHETN-IX-43, 2016.

7 G. Weber, in preparation, U.S. Department of Interior Bureau of Reclamation, Technical Memorandum No. 8540-2019-29, ST-2019-8100-01, 2019.

8 G. Weber, B.J. Merten, J.D. Torrey, "Comparison of Cathodic Disbondment Test Methods for Water Infrastructure Coatings," CORROSION 2018, paper no. 10914 (Houston, TX: NACE, 2018).

9 G. Weber, B.J. Merten, J.D. Torrey, "Impact of Specimen Geometry on Cathodic Disbondment Testing for Protective Coatings," CORROSION 2019, paper no. NACE-2019-13367 (Houston, TX: NACE, 2019).

10 NACE / ASTM G193-12d (2016), "Standard Terminology and Acronyms Relating to Corrosion" (West Conshohocken, PA: ASTM International).

11 A.W. Peabody, *Control of Pipeline Corrosion*, 2nd ed. (Houston, TX: NACE International, 2001), p. 285-295.

12 R.A. Gummow, "Cathodic Protection Potential Criterion for Underground Steel Structures," *Materials Performance* 32 (November 1993): p. 21.

13 W. von Baeckmann, W. Schwenk, W. Prinz, *Handbook of Cathodic Corrosion Protection*, (Houston, TX: Gulf Publishing Company, 1997).

14 L.S. Hou, W. Sun, "Optimal Positioning of Anodes for Cathodic Protection," *SIAM Journal on Control and Optimization* 34, 3 (1996): p. 855.

15 Y. Huang, Z.G. Fang, "Studying on Shielding Effect in the Sacrificial Anode Cathodic Protection System," *Advanced Materials Research* 567 (2012): p. 275.

16 M. Klein, "Photogrammetric Tools for Corrosion Assessment of Reclamation Structures, Part 2," U.S. Department of the Interior Bureau of Reclamation, Technical Memorandum No. 8530-2016-27, 2016.

17 M. Klein, "Photogrammetric Processing from Remotely Operated Vehicle (ROV) Data: Trinity Dam Intake Tunnel," U.S. Department of the Interior Bureau of Reclamation, Technical Memorandum No. 8530-2016-31, 2016.

18 M. Klein, C. Lucero, "Photogrammetric Tools for Condition Assessment of Reclamation Structures," U.S. Department of Interior Bureau of Reclamation, Report No. ST-2015-4413-01, 2015.

19 NACE SP0388 (2014), "Impressed Current Cathodic Protection of Internal Submerged Surfaces of Carbon Steel Water Storage Tanks" (Houston, TX: NACE).

20 P. Taheri, M. Zamanzadeh, "The Science Behind It: Galvanic Cathodic Protection for Power Transimssion Tower Grillage Foundations," *Materials Performance* 55, 12 (2016): p. 30.

Data Sets that Support the Final Report

- T:\Jobs\DO_NonFeature\Science and Technology\2015-PRG-Corrosion Mitigation System Monitoring
- Point of Contact: Jessica Torrey, jtorrey@usbr.gov, 303-445-2376
- Folder includes all data, photographs, reports, and presentations associated with this project.
- Keywords: corrosion, cathodic protection, reference electrode, current shielding, IR drop, hydraulic steel infrastructure, photogrammetry
- Approximate total size of all files: 600 MB

Appendix A – Summary Tables

Table I. Fixed Anode Test Average V_{ON} and V_{OFF} at Representative CSE Positions

Position		$-mV_{ON}$	$-mV_{OFF}$	$-\Delta$	Position		$-mV_{ON}$	$-mV_{OFF}$	$-\Delta$	Position		$-mV_{ON}$	$-mV_{OFF}$	$-\Delta$
	OUT	1214	894	320		OUT	1232	879	353		OUT	1227	885	342
Z10	MID	1178	906	273	**Z4**	MID	1218	887	331	**Z1**	MID	1204	897	307
	IN	1125	916	210		IN	1207	890	317		IN	1163	916	247
Position		$-mV_{ON}$	$-mV_{OFF}$	$-\Delta$	**Position**		$-mV_{ON}$	$-mV_{OFF}$	$-\Delta$	**Position**		$-mV_{ON}$	$-mV_{OFF}$	$-\Delta$
	OUT	1223	897	326		OUT	1239	879	360		OUT	1233	885	348
D10	MID	1201	915	286	**D4**	MID	1228	886	342	**D1**	MID	1220	897	323
	IN	1178	929	249		IN	1221	891	330		IN	1197	912	285
Position		$-mV_{ON}$	$-mV_{OFF}$	$-\Delta$	**Position**		$-mV_{ON}$	$-mV_{OFF}$	$-\Delta$	**Position**		$-mV_{ON}$	$-mV_{OFF}$	$-\Delta$
	OUT	1239	888	351		OUT	1252	875	377		OUT	1251	885	366
H10	MID	1225	906	319	**H4**	MID	1243	885	358	**H1**	MID	1237	892	345
	IN	1209	920	289		IN	1237	883	354		IN	1214	914	300

AVERAGE Applied Potential (V_{ON}):	-1215	+/-	28	mV
AVERAGE Polarized Potential (V_{OFF}):	-897	+/-	15	mV
AVERAGE Difference between V_{ON} and V_{OFF} (Δ):	319	+/-	41	mV

Table II. Moving Anode Test V_{ON} and V_{OFF} Averaged for All Anode Positions at Each CSE Position

Position		$-mV_{ON}$	$-mV_{OFF}$	$-\Delta$	Position		$-mV_{ON}$	$-mV_{OFF}$	$-\Delta$	Position		$-mV_{ON}$	$-mV_{OFF}$	$-\Delta$
Z10	OUT	1019	875	144	**Z4**	OUT	1010	861	149	**Z1**	OUT	998	854	144
	IN	974	865	109		IN	1007	874	133		IN	975	865	110
Position		$-mV_{ON}$	$-mV_{OFF}$	$-\Delta$	**Position**		$-mV_{ON}$	$-mV_{OFF}$	$-\Delta$	**Position**		$-mV_{ON}$	$-mV_{OFF}$	$-\Delta$
D10	OUT	1026	882	144	**D4**	OUT	1008	860	148	**D1**	OUT	997	852	145
	IN	997	866	131		IN	1000	854	146		IN	983	849	134
Position		$-mV_{ON}$	$-mV_{OFF}$	$-\Delta$	**Position**		$-mV_{ON}$	$-mV_{OFF}$	$-\Delta$	**Position**		$-mV_{ON}$	$-mV_{OFF}$	$-\Delta$
H10	OUT	1030	881	149	**H4**	OUT	992	843	149	**H1**	OUT	981	833	148
	IN	997	866	131		IN	995	851	144		IN	974	842	132

AVERAGE Applied Potential (V_{ON}):	-998	+/-	17	mV
AVERAGE Polarized Potential (V_{OFF}):	-860	+/-	14	mV
AVERAGE Difference between V_{ON} and V_{OFF} (Δ):	138	+/-	12	mV

Table III. Summary of V_{ON} and V_{OFF} During Moving Anode Tests Separated by Anode Distance from Gate for IN Position

Position		$-mV_{ON}$	$-mV_{OFF}$	-Δ	Position		$-mV_{ON}$	$-mV_{OFF}$	-Δ	Position		$-mV_{ON}$	$-mV_{OFF}$	-Δ
Z10	0'	971	865	106	**Z4**	0'	1001	875	126	**Z1**	0'	970	867	104
	2'	949	860	89		2'	976	865	111		2'	950	858	92
	4'	945	861	84		4'	968	865	103		4'	944	860	84
	6'	957	867	90		6'	982	876	106		6'	953	865	88
	8'	965	864	101		8'	999	874	126		8'	966	863	103
	10'	1011	870	141		10'	1055	881	174		10'	1015	870	146
Position		**$-mV_{ON}$**	**$-mV_{OFF}$**	**-Δ**	**Position**		**$-mV_{ON}$**	**$-mV_{OFF}$**	**-Δ**	**Position**		**$-mV_{ON}$**	**$-mV_{OFF}$**	**-Δ**
D10	0'	967	867	100	**D4**	0'	978	853	125	**D1**	0'	968	847	121
	2'	964	857	107		2'	968	843	125		2'	956	839	117
	4'	963	856	107		4'	963	842	120		4'	950	840	110
	6'	980	865	115		6'	975	852	124		6'	961	847	114
	8'	991	867	124		8'	992	857	135		8'	976	850	126
	10'	1047	874	173		10'	1052	863	189		10'	1026	858	169
Position		**$-mV_{ON}$**	**$-mV_{OFF}$**	**-Δ**	**Position**		**$-mV_{ON}$**	**$-mV_{OFF}$**	**-Δ**	**Position**		**$-mV_{ON}$**	**$-mV_{OFF}$**	**-Δ**
H10	0'	967	867	100	**H4**	0'	964	855	109	**H1**	0'	947	844	104
	2'	964	857	107		2'	960	845	115		2'	945	836	109
	4'	963	856	107		4'	957	840	117		4'	940	832	108
	6'	980	865	115		6'	975	851	124		6'	956	845	111
	8'	991	867	124		8'	991	851	141		8'	970	842	128
	10'	1047	874	173		10'	1050	857	193		10'	1021	847	173

AVERAGE Applied Potential (V_{ON}):	-979	+/-	30	mV
AVERAGE Polarized Potential (V_{OFF}):	-858	+/-	12	mV
AVERAGE Difference between V_{ON} and V_{OFF} (Δ):	121	+/-	26	mV

Table IV. Summary of V_{ON} and V_{OFF} During Moving Anode Tests Separated by Anode Distance from Gate for OUT Position

Position		-mV$_{ON}$	-mV$_{OFF}$	-Δ	Position		-mV$_{ON}$	-mV$_{OFF}$	-Δ	Position		-mV$_{ON}$	-mV$_{OFF}$	-Δ
Z10	0'	1001	879	122	Z4	0'	998	866	132	Z1	0'	987	858	130
	2'	992	872	120		2'	986	855	131		2'	974	850	124
	4'	985	869	116		4'	977	859	118		4'	967	852	115
	6'	1002	882	120		6'	990	866	124		6'	981	859	122
	8'	1018	882	136		8'	1008	868	140		8'	997	860	137
	10'	1062	873	189		10'	1049	857	192		10'	1035	850	185
Position		**-mV$_{ON}$**	**-mV$_{OFF}$**	**-Δ**	**Position**		**-mV$_{ON}$**	**-mV$_{OFF}$**	**-Δ**	**Position**		**-mV$_{ON}$**	**-mV$_{OFF}$**	**-Δ**
D10	0'	991	878	113	D4	0'	978	861	116	D1	0'	970	854	115
	2'	987	870	117		2'	975	852	122		2'	965	846	120
	4'	985	869	116		4'	970	853	117		4'	960	843	117
	6'	1003	881	122		6'	984	858	127		6'	974	851	123
	8'	1024	885	139		8'	1005	861	144		8'	993	852	141
	10'	1087	893	194		10'	1064	867	197		10'	1050	858	192
Position		**-mV$_{ON}$**	**-mV$_{OFF}$**	**-Δ**	**Position**		**-mV$_{ON}$**	**-mV$_{OFF}$**	**-Δ**	**Position**		**-mV$_{ON}$**	**-mV$_{OFF}$**	**-Δ**
H10	0'	994	884	110	H4	0'	958	850	108	H1	0'	945	834	111
	2'	991	873	118		2'	955	838	117		2'	946	832	114
	4'	989	868	121		4'	953	832	121		4'	942	823	119
	6'	1008	880	128		6'	971	841	130		6'	959	831	128
	8'	1021	877	144		8'	987	843	144		8'	975	829	145
	10'	1092	892	200		10'	1050	848	202		10'	1040	841	199

AVERAGE Applied Potential (V_{ON}):	-995	+/-	35	mV
AVERAGE Polarized Potential (V_{OFF}):	-859	+/-	17	mV
AVERAGE Difference between V_{ON} and V_{OFF} (Δ):	136	+/-	28	mV

Appendix B – Test Gate Drawing

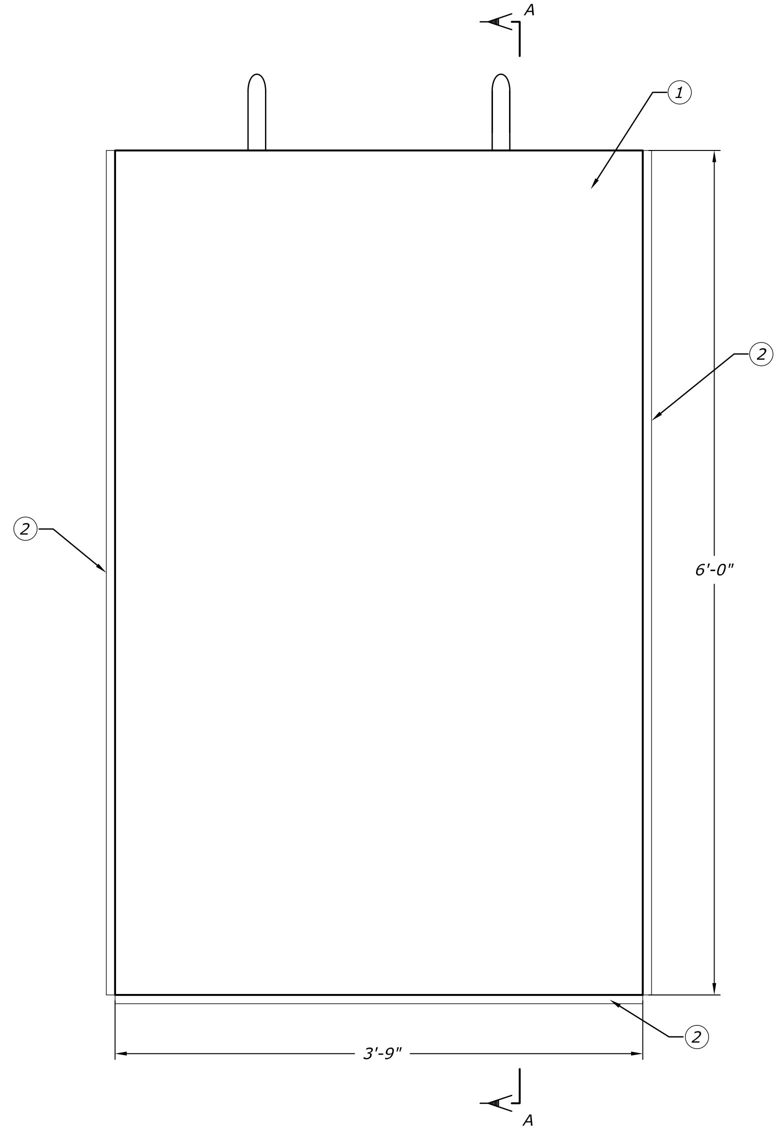

UPSTREAM ELEVATION

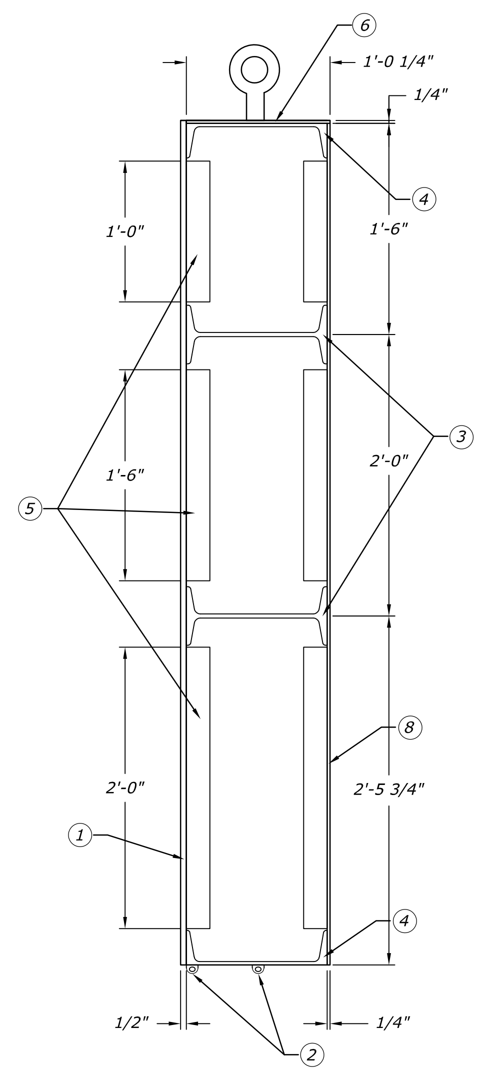

SECTION A-A

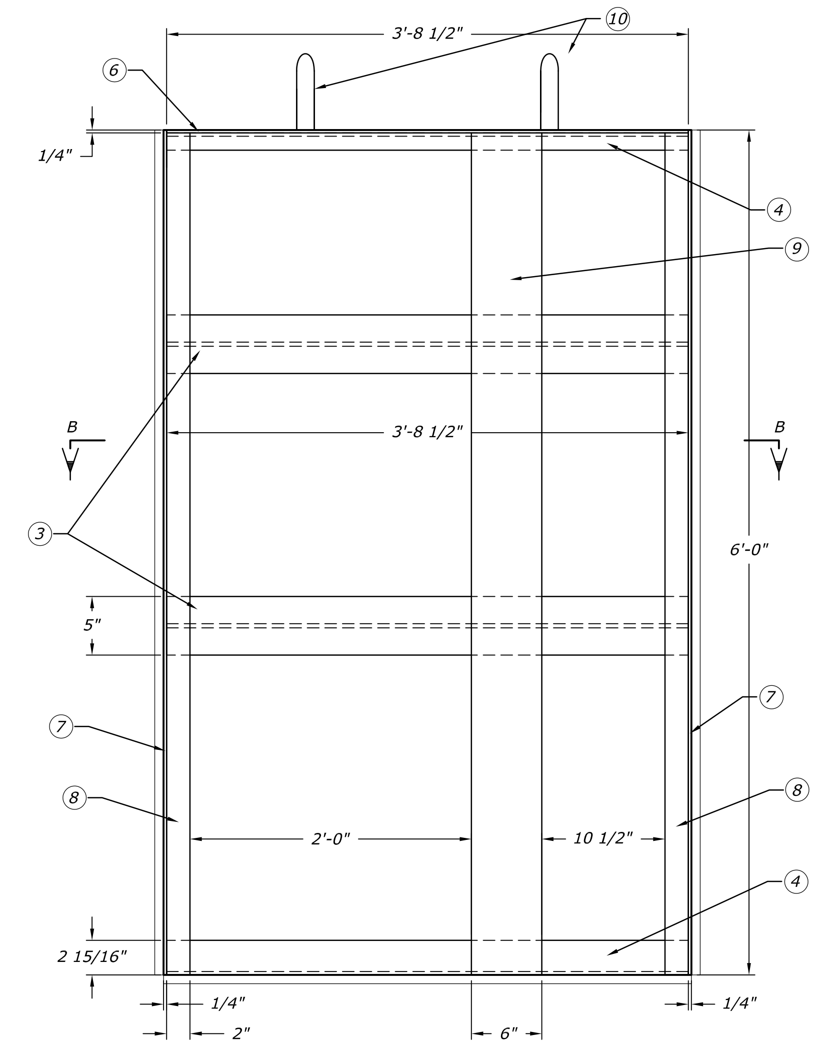

DOWNSTREAM ELEVATION

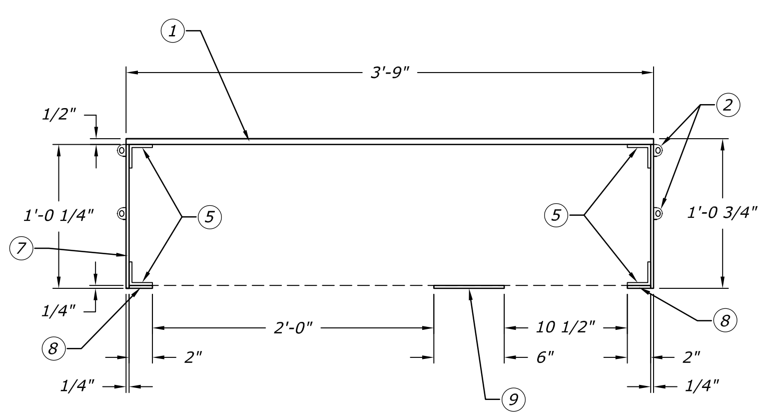

SECTION B-B

LIST OF PARTS

PART NO.	DESCRIPTION	MATERIAL-(ASTM NO.)	QUANTITY	WEIGHT (lbs)
1	Skin plate- 0.5" thick, 45" x 72"	Structural steel-(A36)	1	460
2	Seals- 1" x 1" D-shaped	Foam rubber	32'	NA
3	S 12 x 31.8 beams- 44.5" length	Structural steel-(A36)	2	236
4	C 12 x 20.7 beams- 44.5" length	Structural steel-(A36)	2	154
5	Angle bar- 0.25" thick, 2" x 2" x (12", 18", or 24")	Structural steel-(A36)	4 at each length	58
6	Top plate- 0.25" thick, 12.25" x 44.5"	Structural steel-(A36)	1	39
7	Side plate- 0.25" thick, 12.25" x 72"	Structural steel-(A36)	2	125
8	Side strap- 0.25" thick, 2" x 71.75"	Structural steel-(A36)	2	20
9	Center strap- 0.25" thick, 6" x 71.75"	Structural steel-(A36)	1	31
10	Hoist mechanism- Eyebolts	Galvanized Steel	2	

Total estimated weight of parts 1 thru 9 is 1,123 lbs.

DESIGN NOTES

1. Gate will be secured in flume (w 46.5" x h 72") using 2" wide guides on upstream and downstream side of gate.
2. Hoisting mechanism will be sufficient to lift weight of gate and hold it in a lifted position for an extended period of time.
3. Angle bars (Part #5) will be vertically centered in each compartment.
4. All attachment will be with welds, except hoist mechanism, which may be attached via weld or bolt.
5. All welds will be skip welds so as to create crevices that promote corrosion.
6. Gate will be abrasive blasted and coated with a vinyl coating system.

ALWAYS THINK SAFETY

U.S. DEPARTMENT OF THE INTERIOR
BUREAU OF RECLAMATION

Jessica Torrey
DESIGNED
Jessica Torrey
DRAWN
X
CHECKED
X
TECH. APPR.
X
APPROVED
ADMIN APPROVAL - TITLE

DENVER, CO 2017-01

RESEARCH TEST GATE

FABRICATION DETAILS

UNOFFICIAL

DATE AND TIME PLOTTED
JUNE 26, 2019 13:27
PLOTTED BY
JTORREY

CAD SYSTEM
AutoCAD Rel. 22.0s
CAD FILENAME
TEST GATE.DWG